

Substrate binding and the presence of ferredoxin affect the redox properties of the soluble plant Δ^9 -18:0-acyl carrier protein desaturase

V. Reipa,^a J. Shanklin^b and V. Vilker^a

^a Biotechnology Division, National Institute of Standards and Technology, Gaithersburg MD 20899, USA.
E-mail: vytyas@nist.gov; Fax: 301 975 5449; Tel: 301 975 5056

^b Department of Biology, Brookhaven National Laboratory, Upton, New York, 11973, USA.
E-mail: shanklin@bnl.gov; Fax: 631 344 4407; Tel: 631 344 3414

Received (in Cambridge, MA, USA) 23rd June 2004, Accepted 17th August 2004
First published as an Advance Article on the web 23rd September 2004

Substrate-free Δ^9 -18:0-acyl carrier protein desaturase (abbreviated to Des) [E.C. # 1.14.99.6] was 2-electron reduced with $E^0 = -0.03 + -0.01$ V; the presence of spinach ferredoxin (SpFd) induces an additional 1-electron reduction wave at $E^0 = -0.21 + -0.02$ V, which shifts by 0.106 V upon substrate binding.

In all eukaryotes and some prokaryotes, fatty acid desaturases introduce *cis* double bonds to produce unsaturated fatty acids by performing energy-demanding *syn*-dehydrogenation reactions on methylene-interrupted acyl chains of fatty acids.¹ The soluble plant Δ^9 -18:0-ACP desaturase (Des) is a member of a class of four-helix-bundle diiron enzymes that includes methane monooxygenase and ribonucleotide reductase.² These enzymes bind molecular oxygen, carry out redox chemistry, and use the resulting activated oxygen species to perform oxidation chemistry on their substrates.³ The complex process of introducing a double bond into a fatty acid in a regio- and stereo-specific fashion involves coordinating the binding of a fatty acid substrate, molecular oxygen, and the supply of two electrons necessary for catalysis. The exact catalytic mechanism remains to be determined. However, *in vitro* experiments have shown that substrate binding occurs prior to the enzyme reduction by NAD(P)H via ferredoxin reductase and spinach ferredoxin (SpFd).^{4,5} We therefore initiated experiments to understand the factors that influence the ordering of these processes.

In this communication we report formal potentials for Des in the presence and absence of its physiological redox partner, and in the presence and absence of substrate using the thin layer spectroelectrochemical method.⁶ To our knowledge, Des formal potential data have not been reported previously.

Mature recombinant Des was expressed under the control of the T7 promoter in *E. coli* BL21(DE3) cells. Des was enriched to 90–95% purity by 20CM cation exchange chromatography (Applied Biosystems)[†] and to apparent homogeneity by the passage of the eluate through a G3,000-SW (BioRad) size exclusion column developed with 0.05 mol l⁻¹ HEPES, 0.10 mol l⁻¹ KCl pH 7.0. ACP was expressed and purified as previously described.⁵ 18:0-ACP was synthesized according to Shanklin.⁷ Solutions contained 20 $\mu\text{mol l}^{-1}$ Des per dimer, 40 $\mu\text{mol l}^{-1}$ SpFd, 0.07 mol l⁻¹ KCl, 0.02 mol l⁻¹ HEPES pH 7.0 and a mediator soup (1 $\mu\text{mol l}^{-1}$ each of: Phenazine methosulfate, $E^{\circ} = +0.14$ V; Indigo carmine, $E^{\circ} = -0.125$ V; Phenosafranine, $E^{\circ} = -0.27$ V; Benzyl Viologen, $E^{\circ} = -0.33$ V; and Methyl Viologen, $E^{\circ} = -0.45$ V).

For substrate bound experiments, 18:0-ACP or holo ACP (absent fatty acid) was introduced at stoichiometric (substrate : enzyme = 1 : 1) concentrations. Spectroelectrochemical titrations were conducted using a thin layer cell,⁶ providing exhaustive electrolysis of a sandwiched solution layer. Protein solution absorbance in the 0.1 mm gap between two nano-crystalline Sb-doped tin oxide electrodes was measured parallel to the working electrode surfaces providing a 1 cm optical path-length. Absorbances at several wavelength channels were recorded every 3 mV during the 0.05 mV s⁻¹ linear potential scan. Such a rate allowed sufficient time to stabilize solution potential at each measurement point thus ensuring redox reversibility. Similar redox waves were

obtained during the reverse (oxidative) potential scans, although absorbances gradually diminished due to the slow protein degradation. The decreasing absorbance in the 300 to 400 nm range follows protein reduction in the thin layer cell during the potential ramp from +0.1 to -0.5 V (see Fig. 1 for representative traces) as the μ -oxo bridged iron ions are converted to the ferrous state.⁸

Spectroelectrochemical titrations of Des at 340 nm are shown in Fig. 2. Traces are recorded in the absence (left panel), or presence of 40 $\mu\text{mol l}^{-1}$ SpFd (right panel). In the absence of SpFd, only the redox waves labeled as a and a' are well defined, but in the presence of SpFd, two more waves labeled b and b' become resolved (absorbance variation due to the SpFd reduction was recorded in a separate experiment and subtracted from the total signal). This shows that the interaction of SpFd results in the appearance of a second set of waves at -0.21 and -0.32 in both the presence and absence of substrate. The appearance of reduction waves b, and b' in the presence of the physiological electron donor is reminiscent of that seen with the addition of the small protein "component B" to methane monooxygenase.^{9,10} Formation of the methane monooxygenase–component B complex was shown to alter the structure of the diiron center environment causing a 0.2 V negative reduction potential shift.¹⁰

Des reduction by dithionite, in the absence of its physiological redox partner ferredoxin, has been shown to perform oxidase chemistry (*i.e.*, a 4e⁻ reduction of oxygen to water) rather than the desaturation reaction.^{5,11} It is tempting to speculate that this switch in catalytic outcome is related to the changes in redox waves of the Des we report here in the presence of SpFd.

Redox titration of the substrate-free Des, in the presence of SpFd, at 340 nm (open circles in Fig. 2) shows two redox waves (labeled a and b in Fig. 2 right panel), separated by ~0.3 V. Corresponding ratios of reduced/oxidized protein fractions ($f_{\text{ox}}/f_{\text{red}}$) are plotted on a log scale for each redox wave

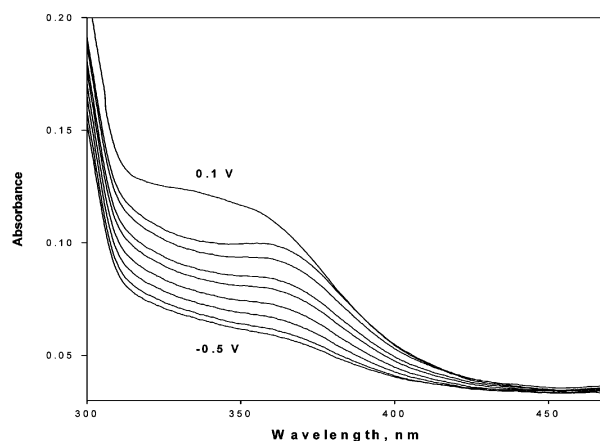


Fig. 1 Δ^9 -18:0-ACP desaturase absorbance spectra sampled during redox potential variation from 0.1 V to -0.5 V relative to standard hydrogen electrode (SHE) at 20 °C in a thin layer cell. Optical path-length 1 cm.

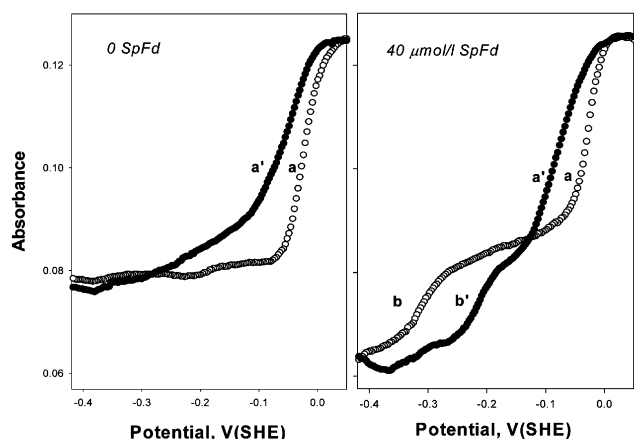


Fig. 2 Absorbance vs. potential plot at 340 nm of substrate-free (○) and 18:0-ACP bound (●) Δ^9 -18:0-ACP desaturase. Left panel curves were recorded in solutions without SpFd, right panel in the presence of SpFd. Spectral contributions from SpFd and mediator soup were subtracted. Letters indicate redox waves as discussed in the text.

in Fig. 3. Formal potentials ($E^{\circ'}$) were determined from the intersection of $\log(f_{\text{ox}}/f_{\text{red}})$ with the abscissa, drawn at $\log(f_{\text{ox}}/f_{\text{red}}) = 0$ for each redox wave. The first redox wave (labeled a in Fig. 2, $E^{\circ'} = -0.03 \pm 0.01$ V, Nernst slope $S = 32 \pm 3$ mV) is characteristic of a 2-electron charge transfer reaction. SpFd addition induces an additional redox wave at -0.32 ± 0.02 V (b in Figs. 2, 3), and is attributed to a 1-electron process ($S = 56 \pm 4$ mV). Assuming that absorbance decrease is proportional to the number of iron ions reduced, this suggests that a total of 3 electrons are transferred to diiron dimer. However, this number can be considered preliminary pending investigation by a method better suited to quantitation.

Introduction of a stoichiometric amount of 18:0-ACP substrate results in detectable changes to both redox waves (full circles in Fig. 2). First, the SpFd-induced redox wave occurs at $E = -0.21 \pm 0.02$ V as a result of a 0.106 V formal potential shift in the positive direction (compare b with b' in Fig. 2). Such a shift significantly increases the driving force for electron transfer between SpFd ($E^{\circ'} \sim \text{minus}0.4$ V) and the Des. Second, the 2-electron reaction at $E^{\circ'} = -0.03$ V turns into a composite of two 1-electron waves with midpoint at $E^{\circ'} = -0.08$ V, as indicated by $S = 53 \pm 6$ mV (see a' in Fig. 3).

A substrate-induced 0.106 V positive shift of the formal reduction potential upon binding of substrate to the Des has precedent in the cytochrome P450cam system,^{6,12} and suggests catalytic cycle redox control by substrate binding.

Switching from 2-electron to single electron transfer reactions upon substrate binding (compare redox waves a, a' in Fig. 3) could be related to the previously reported substrate-induced conformational change of the diiron center.² Structural data show that 18:0-ACP substrate was predicted to reside closer to one of two active site iron atoms.² In addition, formation of one four-coordinate and one five-coordinate iron ion in the reduced enzyme-substrate complex was demonstrated by magnetic circular dichroism (MCD) spectroscopy.¹³ Asymmetric substrate interaction could explain the 20–30 mV formal potential difference between the two cluster iron ions suggested by the apparently sigmoidal Nernst plot seen for wave a' (Fig. 3). Although a mixed valence state for Des was not detected by electron paramagnetic resonance spectroscopy (EPR) above 240 K,¹⁴ the data presented here suggest that a mixed valence state should be stabilized for the substrate-bound Des.

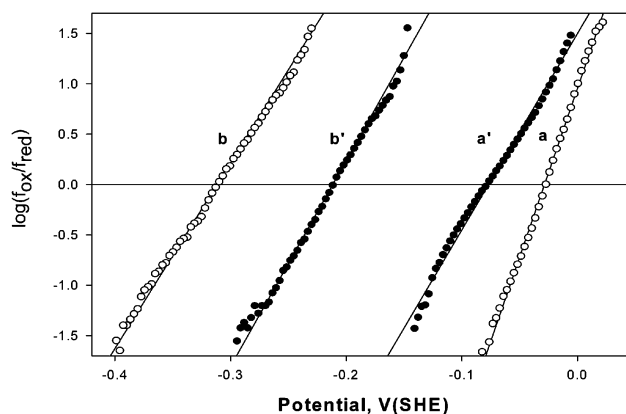


Fig. 3 Nernst plots of Δ^9 -18:0-ACP desaturase redox waves as labeled on Fig. 2. Fraction of the reduced species was calculated from the absorbance reading at 340 nm. Intersections with abscissa drawn as $\log(f_{\text{red}}/f_{\text{ox}}) = 0$ were used to estimate potential values.

In summary, we have demonstrated that Des formal potential is highly sensitive to the presence of its biological redox partner SpFd and to the binding of 18:0-ACP substrate. Substrate-free enzyme becomes 2-electron reduced with $E^{\circ'} = -0.03 \pm 0.01$ V, the addition of SpFd results in the appearance of an additional 1-electron reduction wave at $E^{\circ'} = -0.32 \pm 0.02$ V. Formal potential of this redox process is shifted to $E^{\circ'} = -0.21 \pm 0.02$ V upon 18:0-ACP substrate binding to Des, suggesting thermodynamic redox gating of the enzymatic cycle analogous to that seen for cytochrome P450s oxygenases.¹²

JS thanks the Office of Basic Energy Sciences of the U.S. Department of Energy for financial support.

Notes and references

† Certain commercial equipment, instruments, and materials are identified in this paper to specify adequately the experimental procedure. In no case does such identification imply recommendation or endorsement by the National Institute of Standards and Technology, nor does it imply that the material or equipment is necessarily the best available for the purpose.

- J. Shanklin and E. B. Cahoon, *Ann. Rev. Plant Physiol. Plant Mol. Biol.*, 1998, **49**, 611.
- Y. Lindqvist, W. Huang, G. Schneider and J. Shanklin, *EMBO J.*, 1996, **15**, 4081; Y. Lindqvist, W. Huang, G. Schneider and J. Shanklin, *Protein Expression Purif.*, 1999, **15**, 314.
- P. H. Buist, *Nat. Prod. Rep.*, 2004, **2**, 249.
- K. S. Lyle, J. A. Haas and B. G. Fox, *Biochemistry*, 2003, **42**, 5857.
- J. A. Broadwater, C. Achim, E. Münck and B. G. Fox, *Biochemistry*, 1999, **38**, 12197.
- V. Reipa, M. P. Mayhew, M. J. Holden and V. L. Vilker, *Chem. Commun.*, 2002(4), 318.
- J. Shanklin, *Protein Expression Purif.*, 2000, **18**, 355.
- B. G. Fox, J. Shanklin, C. Somerville and E. Münck, *Proc. Natl. Acad. Sci. USA*, 1993, **90**, 2486.
- K. E. Liu and S. J. Lippard, *J. Biol. Chem.*, 1991, **266**, 12836.
- K. E. Paulsen, Y. Liu, B. G. Fox, J. D. Lipscomb, E. Münck and M. T. Stankovich, *Biochemistry*, 1994, **33**, 713.
- J. A. Broadwater, J. Ai, T. M. Loehr, J. Sanders-Loehr and B. G. Fox, *Biochemistry*, 1998, **37**, 14664.
- S. G. Sligar and I. C. Gunsalus, *Proc. Natl. Acad. Sci. USA*, 1976, **73**, 1078.
- E. I. Solomon, *Inorg. Chem.*, 2001, **40**, 3656.
- R. Davydov, B. Behrouzian, S. Smoukov, B. M. Hoffman and J. Shanklin (2004, in preparation).